AGU PUBLICATIONS

JGR

Journal of Geophysical Research: Oceans

RESEARCH ARTICLE

10.1002/2016JC012228

Evolution of the East Greenland Current from Fram Strait to Denmark Strait: Synoptic measurements from summer 2012

L. Håvik[1], R. S. Pickart[2], K. Våge[1], D. Torres[2], A. M. Thurnherr[3], A. Beszczynska-Möller[4], W. Walczowski[4], and W.-J. von Appen[5]

[1]Geophysical Institute, University of Bergen and Bjerknes Centre for Climate Research, Bergen, Norway, [2]Woods Hole Oceanographic Institution, Woods Hole, Massachusetts, USA, [3]Lamont-Doherty Earth Observatory, Palisades, New York, USA, [4]Institute of Oceanology Polish Academy of Sciences, Sopot, Poland, [5]Helmholtz Centre for Polar and Marine Research, Alfred Wegener Institute, Bremerhaven, Germany

Key Points:
- Two summer 2012 shipboard surveys document the evolution of the East Greenland Current (EGC) system from Fram Strait to Denmark Strait
- The water mass and kinematic structure of the three distinct EGC branches are described using high-resolution measurements
- Transports of freshwater and dense overflow water have been quantified for each branch

Correspondence to:
L. Håvik,
lisbeth.havik@uib.no

Citation:
Håvik, L., R. S. Pickart, K. Våge, D. Torres, A. M. Thurnherr, A. Beszczynska-Möller, W. Walczowski, and W.-J. von Appen (2017), Evolution of the East Greenland Current from Fram Strait to Denmark Strait: Synoptic measurements from summer 2012, *J. Geophys. Res. Oceans*, *122*, 1974–1994, doi:10.1002/2016JC012228.

Received 11 AUG 2016
Accepted 11 FEB 2017
Accepted article online 15 FEB 2017
Published online 13 MAR 2017

Abstract We present measurements from two shipboard surveys conducted in summer 2012 that sampled the rim current system around the Nordic Seas from Fram Strait to Denmark Strait. The data reveal that, along a portion of the western boundary of the Nordic Seas, the East Greenland Current (EGC) has three distinct components. In addition to the well-known shelfbreak branch, there is an inshore branch on the continental shelf as well as a separate branch offshore of the shelfbreak. The inner branch contributes significantly to the overall freshwater transport of the rim current system, and the outer branch transports a substantial amount of Atlantic-origin Water equatorward. Supplementing our measurements with historical hydrographic data, we argue that the offshore branch is a direct recirculation of the western branch of the West Spitsbergen Current in Fram Strait. The total transport of the shelfbreak EGC (the only branch sampled consistently in all of the sections) decreased toward Denmark Strait. The estimated average transport of dense overflow water ($\sigma_\theta > 27.8$ kg/m^3 and $\theta > 0$°C) in the shelfbreak EGC was 2.8 ± 0.7 Sv, consistent with previous moored measurements. For the three sections that crossed the entire EGC system the freshwater flux, relative to a salinity of 34.8, ranged from 127 ± 13 to 81 ± 8 mSv. The hydrographic data reveal that, between Fram Strait and Denmark Strait, the core of the Atlantic-origin Water in the shelfbreak EGC cools and freshens but changes very little in density.

1. Introduction

The East Greenland Current (EGC) is a major pathway for transporting freshwater from the Arctic Ocean to the North Atlantic [*Haine et al.*, 2015], as well as an important supplier of dense overflow water to Denmark Strait [*Strass et al.*, 1993; *Jochumsen et al.*, 2012; *Harden et al.*, 2016]. Numerous studies have focused on the EGC in both Fram and Denmark Straits; however, the region in between has only been sparsely observed and the along-stream evolution of the current remains largely unexplored. As water exits the Arctic Ocean in the EGC through Fram Strait, it is supplemented by a cross-strait flux of warm and saline water emanating from the West Spitsbergen Current (WSC). These recirculating waters, which originate from the North Atlantic via the Norwegian Atlantic Current, enhance the annual mean volume transport of the EGC by at least 3 Sv, resulting in a total southward transport of 8.7 Sv at 78°50′N [*de Steur et al.*, 2014].

Downstream of Fram Strait, *Woodgate et al.* [1999] estimated the transport of the EGC from a mooring array deployed across the current at 75°N in 1994–1995. They found a throughput of 8 ± 1 Sv, with no apparent seasonal signal. Farther south, the volume transport of the current gradually decreases as water is diverted into the Jan Mayen Current [*Bourke et al.*, 1992] and the East Icelandic Current [*Macrander et al.*, 2014] (Figure 1). At the northern end of the Blosseville Basin, the EGC bifurcates into two distinct branches: the shelfbreak EGC and the separated EGC. The former continues southward along the east Greenland shelfbreak, while the latter veers offshore and follows the base of the Iceland slope toward Denmark Strait [*Våge et al.*, 2013; *Harden et al.*, 2016]. While the Jan Mayen and East Icelandic Currents flow into the interior of the Greenland and Iceland Seas, respectively, the two branches of the EGC in the Blosseville Basin pass through Denmark Strait into the North Atlantic.

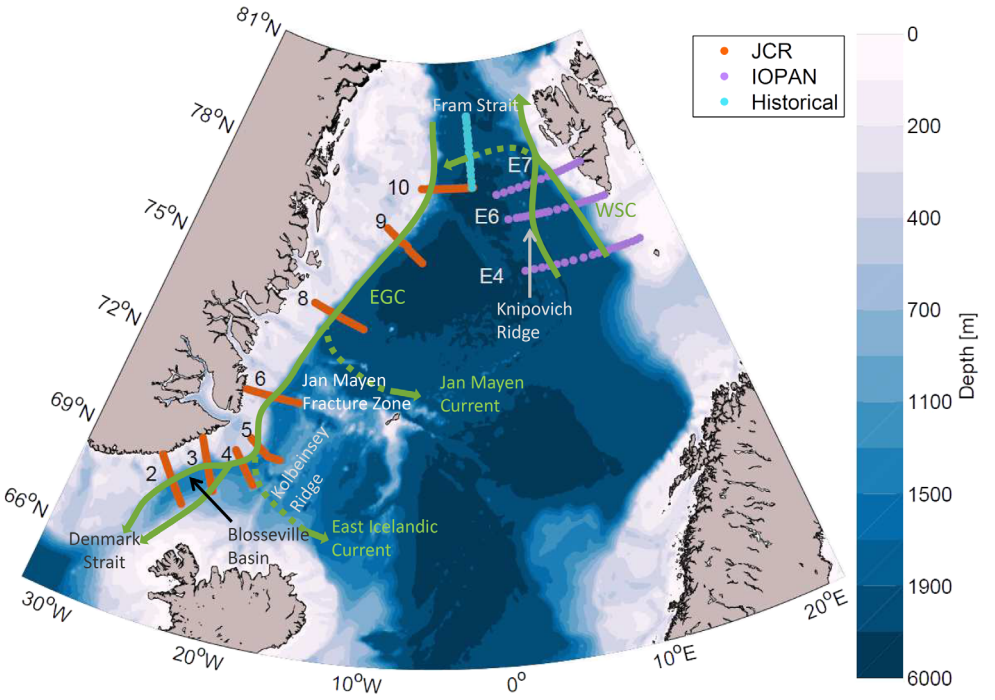

Figure 1. Location of the sections occupied during the two shipboard surveys in summer 2012 and the composite meridional section obtained from historical data in Fram Strait. The main currents discussed in the Introduction are sketched in green. In the Blosseville Basin, the EGC bifurcates into the shelfbreak branch and the separated branch. Bathymetric features and geographical locations discussed in the text are indicated on the map. The bathymetry was obtained from the 2 min resolution Etopo2 product.

The export of dense overflow water from the Nordic Seas contributes to the deep limb of the Atlantic Meridional Overturning Circulation. Approximately half of this export takes place through Denmark Strait [*Hansen and Østerhus*, 2000], and more than two thirds of that is associated with the EGC [*Harden et al*., 2016]. Hence, knowledge of the upstream evolution of the current is essential for understanding the processes that dictate the supply of dense overflow water to Denmark Strait. *Mauritzen* [1996] concluded that Atlantic Water modified along the perimeter of the Nordic Seas is the main contributor to the overflow water that enters the strait via the EGC. This warm-to-cold conversion takes place predominantly in the northeastern Nordic Seas, due to strong buoyancy forcing in that region [*Isachsen et al*., 2007]. On the other hand, *Strass et al*. [1993] argued that as much as half of the transport of dense overflow water through Denmark Strait can be formed by isopycnal mixing between the recirculated Atlantic-origin Water in the EGC and the interior waters of the Greenland Sea. However, this mechanism may exhibit large interannual variability and the transport estimates are based on particular assumptions about the structure of the velocity field.

The surface layer of the EGC has a high freshwater content due to its origin in the Arctic Ocean, as well as from seasonal ice melt in the Nordic Seas and Fram Strait [*Rudels et al*., 2002]. The composition of the freshwater has been examined both from transects across the EGC from Fram Strait to Denmark Strait [*de Steur et al*., 2015] and within Fram Strait itself from a combination of in situ measurements and an inverse model [*Rabe et al*., 2013]. However, due to a lack of velocity measurements, only a few estimates of the EGC freshwater transport are available. *Holfort and Meincke* [2005] obtained a total (liquid and solid) freshwater transport of 40–55 mSv relative to a reference salinity of 34.9 from moorings deployed on the east Greenland shelf close to 74°N in 2001–2002. Using data from the 2002 RV Oden expedition, *Nilsson et al*. [2008] estimated an average freshwater flux of 60 mSv. They concluded that the freshwater was largely conserved in the EGC as it progressed from north of Fram Strait to south of Denmark Strait. A decade of moored observations in Fram Strait indicated that the EGC has a relatively constant annual mean liquid freshwater flux of 40 mSv [*de Steur et al*., 2009]. Based on model results, *de Steur et al*. [2009] estimated an additional flux of freshwater on the Greenland shelf of 26 mSv—emphasizing that the sparse measurements on the wide shelf could lead to an underestimate of the flux. *Rabe et al*. [2009] concluded that a considerable part of the

freshwater transport through Fram Strait took place on the shelf rather than along the slope, and estimated a mean transport from three summer sections of 80 ± 6 mSv. An overview of the freshwater fluxes east of Greenland can be found in *Holfort et al*. [2008].

To date, there have been relatively few high-resolution transects—especially with velocity measurements—across the EGC in the Nordic Seas, partly because of the presence of pack ice (see *Seidov et al*. [2015, Figure 4] for an overview of the historical data). *Seidov et al*. [2015] calculated climatologies of temperature and salinity on a 0.25° × 0.25° grid for the Nordic Seas to investigate decadal variability of hydrographic properties. However, it is clear that variability on short time and space scales cannot be assessed from such a climatological data assembly. Numerical models are very powerful tools for evaluating ocean variability, water mass transformation, and current pathways. Most models capture the southward transport along the coast of east Greenland, but, in order to resolve the more subtle features, fairly high resolution is required. The model employed by *Bacon et al*. [2014] of the East Greenland Coastal Current (EGCC) south of Denmark Strait has a resolution of 1/12°, corresponding to around 5 km. They conclude that this is sufficient to resolve the EGCC which typically has a width between 15 and 20 km. Unfortunately, their analysis only covers the east Greenland shelf south of Denmark Strait. North of Denmark Strait, *Köhl et al*. [2007] presented results from a model with a resolution of 1/10°. Their focus was on the water masses contributing to the Denmark Strait Overflow Water, and no detailed description of the EGC was provided. As pointed out in *Bacon et al*. [2014], it is important to validate the model output against observations, in particular in this region where there are still many uncertain aspects regarding the circulation and water masses.

Only two previous cruises have sampled the EGC from Fram Strait to Denmark Strait as part of a single survey. In fall 1998, five sections across the EGC were measured by RV Polarstern. A detailed description of the hydrographic properties of the water masses that constitute the EGC is presented in *Rudels et al*. [2002], but no velocity measurements or transport estimates are discussed. In 2002, RV Oden traversed the East Greenland Current 5 times within the same region. Their focus was on the along-stream changes in the water mass characteristics based on hydrographic and chemical measurements [*Rudels et al*., 2005; *Jeansson et al*., 2008]. The velocity measurements obtained were primarily used to calculate freshwater fluxes [*Nilsson et al*., 2008]. As such, no previous studies have robustly characterized the kinematic structure of the current nor estimated its along-stream changes in volume transport.

In this study, we use a set of eight high-resolution shipboard transects across the EGC occupied during summer 2012 from Fram Strait to Denmark Strait to investigate the along-stream evolution of the current, its velocity and water mass structure, and the transport of both freshwater and dense overflow water. To address the importance of the recirculating Atlantic-origin Water in Fram Strait to the EGC system, we use three sections of the WSC occupied during the same summer, as well as historical data from the strait itself. We demonstrate that the EGC is in fact a system of distinct branches, from the inner shelf to the outer slope, which undergo significant modification as they progress equatorward in the Nordic Seas.

2. Data and Methods

2.1. East Greenland Current

The EGC data set was collected on a survey carried out on the RRS James Clark Ross, which began in Denmark Strait in late July and ended in Fram Strait in late August 2012. Here we use eight transects across the east Greenland shelf and slope (Figure 1), with particular emphasis on section 10 in the southern Fram Strait, section 6 along the Jan Mayen Fracture Zone, and section 3 in the Blosseville Basin. These three sections are representative of the general hydrographic structure and kinematic features of the current system between Fram Strait and Denmark Strait. The distance between stations was typically 5–7 km, which is close to the Rossby radius of deformation in this region (approximately 5 km) [*Nurser and Bacon*, 2014].

A Sea-Bird 911+ conductivity-temperature-depth (CTD) instrument was mounted on a rosette containing twelve 10 L Niskin bottles. Downcast profiles of temperature and salinity were averaged into 2 db bins, from which other variables were computed. The accuracy of the CTD measurements was 0.3 db for pressure, 0.001°C for temperature, and 0.002 for salinity [*Våge et al*., 2013]. Velocity profiles were obtained at

each site using a lowered acoustic Doppler current profiler (LADCP) system attached to the rosette, consisting of upward-facing and downward-facing RDI 300 kHz instruments. An updated version of the barotropic tidal model of *Egbert and Erofeeva* [2002], with a resolution of 1/60°, was used to detide the velocity data before they were rotated into along-section and across-section components. The uncertainty in the tidal model is mostly related to its representation of the bathymetry. We estimate this error by comparing the model bathymetry to the measured bathymetry and scale this ratio by the tidal velocity. The tidal currents were strongest in the southern sections, particularly in section 2, where this resulted in an error of approximately 2 cm/s. Conservatively, we use this value for all sections although the model likely performs slightly better farther north.

Vertical sections of potential temperature, salinity, and velocity were constructed by interpolation onto a regular grid with a resolution of 10 m in the vertical and 3 km in the horizontal using a Laplacian-spline routine [*Pickart and Smethie*, 1998]. Absolute geostrophic velocity sections were calculated by referencing the geostrophic shear obtained from the gridded hydrography using similarly gridded detided velocities from the LADCP. The mean values of the relative and directly measured velocities were matched between 50 m and the bottom for each gridded profile. Velocity error estimates were calculated following the method outlined in *Sutherland* [2008]. This method combines the errors from the detiding routine and ageostrophic effects such as baroclinic tides in a root-sum-square fashion. The error is reduced by the square root of the number of station pairs covering the current branch in question (equivalent to number of degrees of freedom). With this method the error increases if the station spacing is large and the width of the current is narrow, i.e., where the current is resolved by only a few stations. This resulted in typical velocity errors of 1–3 cm/s.

The freshwater transport (FWT) for each section was calculated as

$$FWT = \int_E^W \int_{z=S_{ref}}^{z=0} AGV(x,z) \cdot \frac{S_{ref} - S(z)}{S_{ref}} dz dx; \quad (1)$$

where S_{ref} is the reference salinity of 34.8 (same as that used in *Våge et al*. [2013]), AGV is the absolute geostrophic velocity, and E and W correspond to the eastern and western ends of each gridded section, respectively. Error estimates for volume transport were obtained by multiplying the error velocity by the area of the current. For the FWT, this number was reduced by the amount of freshwater present, expressed by the fraction in equation (1).

2.2. West Spitsbergen Current and Fram Strait

We also use data from a hydrographic/velocity survey conducted in summer 2012 by the Institute of Oceanology, Polish Academy of Sciences (IOPAN) in the northeastern part of the boundary current system of the Nordic Seas. In particular, three sections are used that were occupied in and south of Fram Strait (see Figure 1). The cruise took place roughly 1 month earlier than the EGC survey. A similar setup was used consisting of a Sea-Bird 911+ CTD mounted on a 12-bottle rosette with 12 L bottles (only 9 bottles were used in order to make room for the LADCP). The temperature and pressure sensors underwent precruise and postcruise laboratory calibrations, and the conductivity sensors were calibrated using the in situ water sample data. The errors were estimated as 1 db for pressure, 0.001°C for temperature, and 0.002 for salinity.

A single downward-facing RDI 300 kHz LADCP was used to obtain vertical profiles of horizontal velocity. This resulted in limited data coverage in the upper 50 m, and, due to large instrument tilts during the casts, there were some instances of data gaps at depth. Nonetheless, the overall data quality was good, and the velocity profiles were detided using the same model employed for the EGC profiles. The CTD data from the IOPAN survey were gridded, and the geostrophic velocities referenced, in the same fashion as the data from the EGC, except with a horizontal grid spacing of 5 km due to the coarser station spacing. Note that sections E7 and 10 in the southern Fram Strait were approximately along the same latitude (Figure 1), and the combination of these resulted in a complete transect across the strait.

To complement our analysis of the boundary current system of the Nordic Seas, we collected historical CTD data from meridional sections in Fram Strait obtained during summers 1997–1999 and 2002–2004 from the PANGAEA database [*Hansen*, 2006a,2006b,2006c; *Schauer and Budéus*, 2010; *Schauer*, 2010; *Schauer and Rohardt*, 2010]. The hydrographic variables for each of the meridional sections were gridded using the same interpolation scheme with a resolution of 0.1° latitude and 10 m in the vertical. Due to the lack of direct

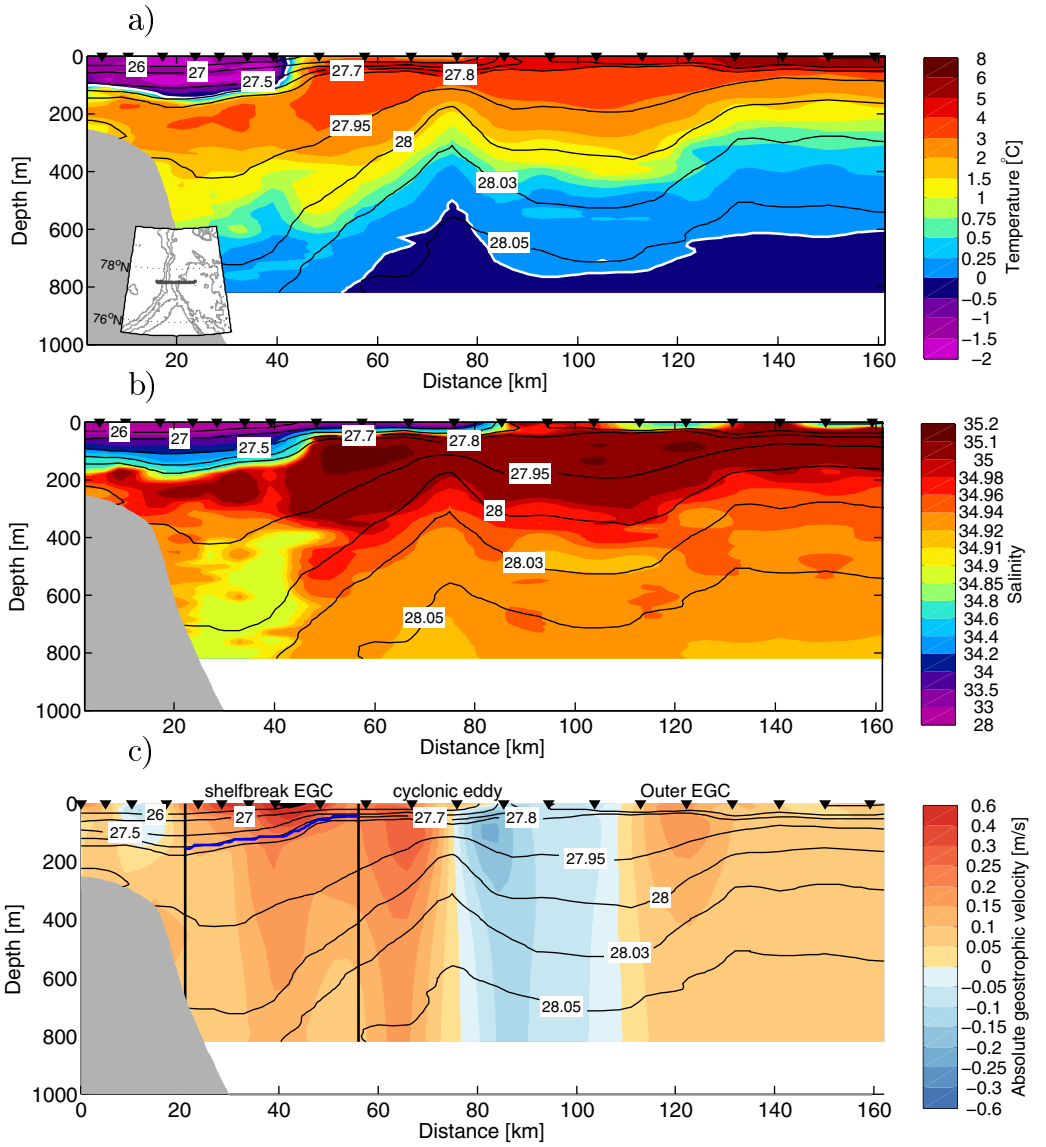

Figure 2. Vertical sections of (a) potential temperature, (b) salinity, and (c) absolute geostrophic velocity with contours of potential density (kg/m^3), for section 10 in Fram Strait. The location of the section is shown in the inset in Figure 2a. Positive velocities are toward the south. The black inverted triangles along the top of each figure indicate the station locations. The white contours in Figure 2a represent the 0°C isotherms. The black vertical lines in Figure 2c enclose the shelfbreak branch of the EGC (see the text for details on how this branch was defined). The blue contour in Figure 2c is the 27.7 kg/m^3 isopycnal which separates the surface layer from the intermediate layer. The different kinematic features present in the section are identified along the top of Figure 2c.

velocity measurements, we calculated geostrophic velocities from the hydrography relative to a level of no motion at 1000 m for these sections.

3. Hydrographic Structure of the East Greenland Current

In every crossing of the east Greenland shelf and slope, the hydrography of the EGC had a three-layered structure. This is illustrated nicely by the temperature and salinity fields from section 10 (Fram Strait), section 6 (Jan Mayen Fracture Zone), and section 3 (Blosseville Basin) (first two parts of Figures 2, 3, and 4, respectively). The surface layer consists of fresh Polar Surface Water (PSW) extending all the way across most of the sections. In the upper few meters, this layer is warmer due to summer insolation, but the temperature rapidly decreases below that. The outermost station on section 9 and the stations offshore of approximately x = 85 km on section 10 were the only ones without this fresh surface layer. On the shelf, the

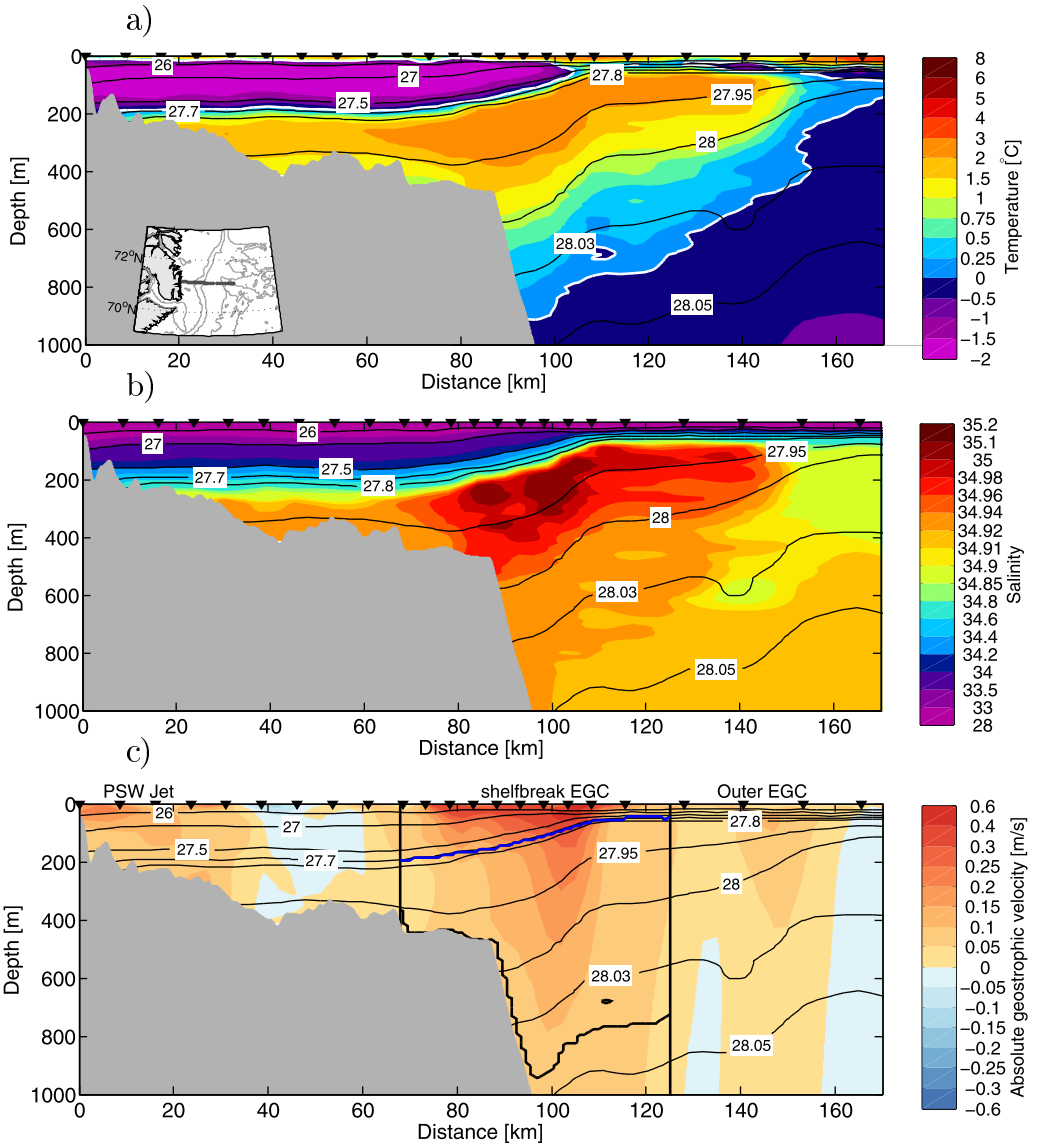

Figure 3. Vertical sections of hydrography and velocity for section 6 near the Jan Mayen Fracture Zone, otherwise as Figure 2. The lower limit for the Atlantic-origin Water in the shelfbreak EGC is marked by the thick black contour (section 10 did not extend deep enough to capture this).

surface layer is roughly 150–200 m thick, becoming as thin as 50 m offshore. This results in a pronounced upward tilt of the isopycnals toward the east.

Immediately below the PSW is the warmer and saltier Atlantic-origin Water. This is broadly defined as all intermediate waters with a temperature above 0°C [*Våge et al.*, 2011]. At the two northernmost sections, the Atlantic-origin Water could be separated into two distinct components: the warm and saline Atlantic Water originating directly from the WSC in Fram Strait, and the colder and less saline Arctic Atlantic Water that is generally situated deeper on the east Greenland slope [*Rudels et al.*, 2002]. The latter enters the Arctic Ocean via the WSC or through the Barents Sea and is modified while flowing through the Arctic Ocean before exiting Fram Strait in the EGC. South of section 9, these two water masses were difficult to distinguish. *Rudels et al.* [2005] referred to the combination of the two Atlantic-origin Water masses as Return Atlantic Water but we will refer to the mixture simply as Atlantic-origin Water. The Atlantic-origin layer is characterized by an intermediate maximum in temperature and salinity and is typically 500–700 m thick. Below this, i.e., below the deep 0°C isotherm, resides the colder and less saline lower intermediate layer.

The water masses at the offshore ends of the transects differed north and south of the Jan Mayen Fracture Zone. In the Greenland Sea, the Atlantic-origin Water was present across the entire sections with a

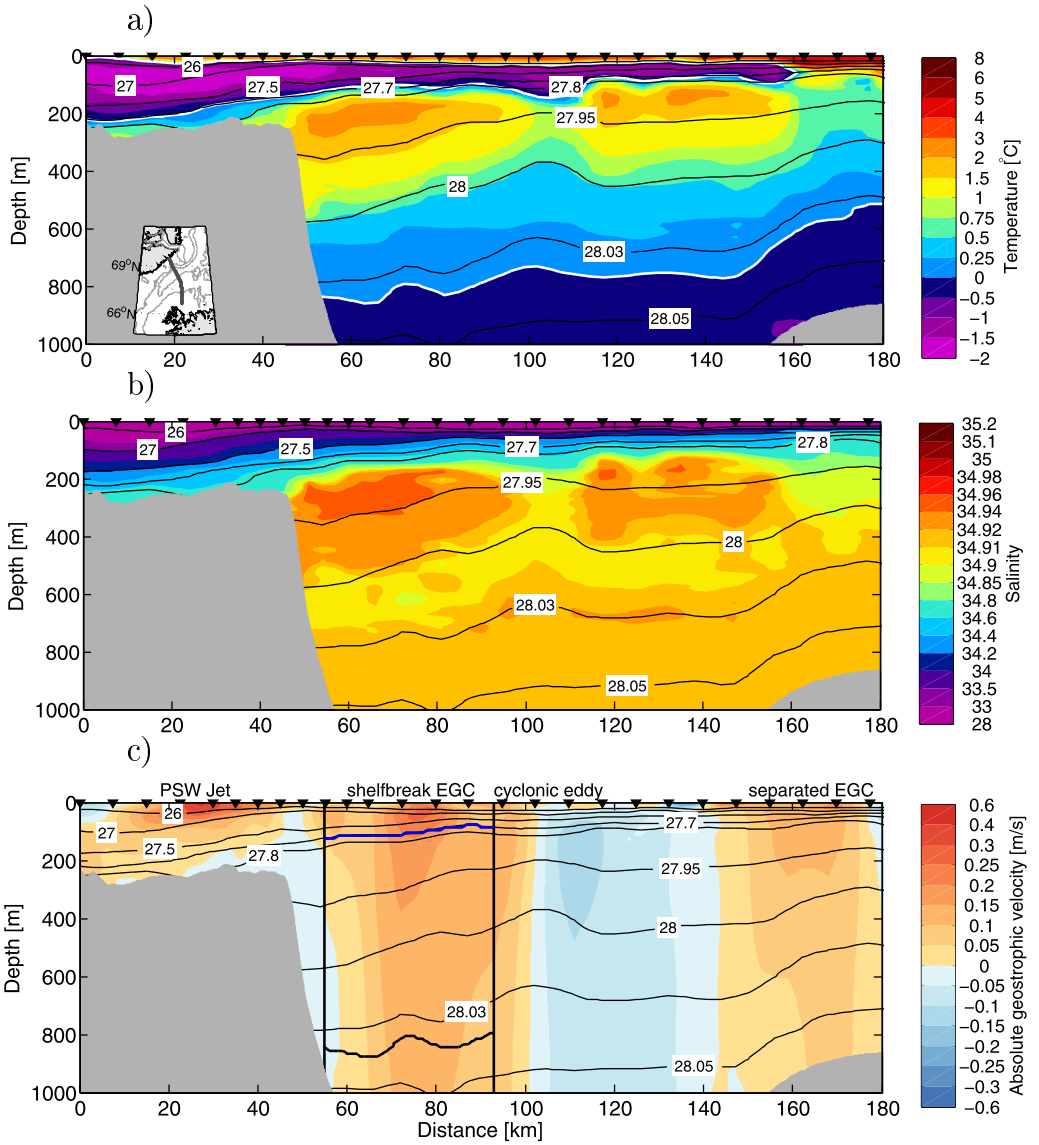

Figure 4. Vertical sections of hydrography and velocity for section 3 in the Blosseville Basin, otherwise as Figure 3.

clear intermediate salinity and temperature maximum. From section 6 and southward, however, the offshore water mass was less saline and colder, quite distinct from the Atlantic-origin Water (note the fresher water between 50 and 400 m at the outer two stations in Figure 3b). We generically refer to the waters offshore of the Atlantic-origin Water as ambient water, even though the characteristics differed from section to section.

In addition to distinguishing the water masses in terms of their potential temperature/salinity (θ/S) characteristics, we divided the surface and intermediate waters by the 27.7 kg/m^3 isopycnal following *Rudels et al.* [2002]. This is a broader definition than the above separation into PSW and intermediate Atlantic-origin Water, which was useful offshore of the EGC system where the θ/S properties did not allow for an easy classification of the water masses. Within the EGC, where the boundary between the PSW and the Atlantic-origin Water was sharp, the density definition to a large degree coincides with the θ/S definition (see e.g., Figure 3b). *Rudels et al.* [2002] further separated the intermediate layer from the deep waters by the $\sigma_{0.5} = 30.444$ kg/m^3 isopycnal. However, due to the limited sampling at depth in the northernmost sections, we focus the analysis on the intermediate waters down to the deep 0°C isotherm.

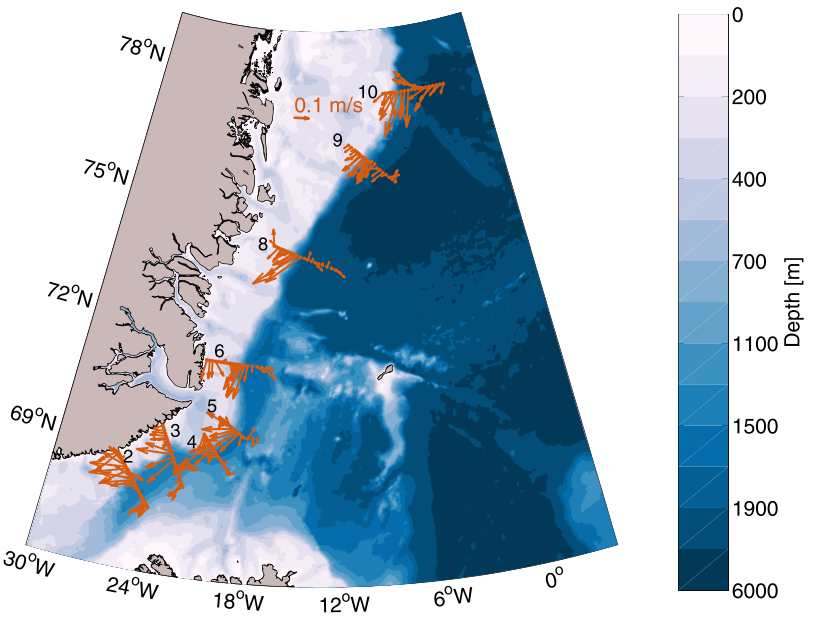

Figure 5. Depth-integrated velocity vectors for the upper 500 m at each station. For stations at shallower depths the integration was made to the bottom.

4. Velocity Structure of the East Greenland Current

As an overview of the current structure adjacent to Greenland, we show the depth-integrated LADCP vectors from the surface to 500 m for each station (Figure 5). At the locations where the bottom depth was shallower than 500 m, the integration was made to the bottom. In general, the highest velocities in each section are found in the vicinity of the shelfbreak and upper continental slope. However, note that there is strong flow on the inner shelf for those crossings that extended close to the Greenland coast (sections 2, 3, and 6). In addition, there are instances of large velocities well seaward of the shelfbreak (e.g., sections 2 and 9).

Inspection of the vertical sections of absolute geostrophic velocity reveals that the EGC can be considered a system of distinct branches. North of 71°N there is an offshore velocity core that we refer to as the outer EGC. This was observed in sections 10, 9, and 6 (see the bottom of Figures 2 and 3). In section 10, it was associated with a pronounced thinning of the Atlantic-origin layer, while at sections 9 and 6 it coincided with the transition from the Atlantic-origin Water to the ambient water farther offshore. In all cases, the current was supported by a density front (upward-sloping isopycnals in the offshore direction). There is also a well-defined jet on the shelf that was present on the transects that extended close to the Greenland coast (sections 6, 3, and 2; see Figures 3 and 4). This is termed the PSW Jet and is also associated with a density front, in this case due to a thinning of the cold and fresh surface layer. The presence of both the outer EGC and the PSW Jet was mentioned by *Nilsson et al.* [2008]. However, they did not elaborate on the importance or implications of these separate components, and made no quantitative estimates of their transports. Finally, there is enhanced equatorward flow in the vicinity of the shelfbreak on all of the transects. Keeping with the nomenclature introduced by *Våge et al.* [2013], this jet is referred to as the shelfbreak EGC. Immediately offshore of that the flow was weaker and at times reversed.

In the southern part of the domain, specifically in sections 2 and 3 within the Blosseville Basin, the separated EGC was readily identifiable as a surface-intensified current centered over the base of the Iceland slope. These various kinematic components of the boundary current system were manifest differently from section to section (see e.g. the bottom of Figures 2–4). In addition, mesoscale eddies were sampled on some of the sections. Due to this variability, an objective measure for delimiting each of the current branches was difficult to obtain; hence, they were subjectively distinguished using their hydrographic and velocity structure as detailed below. The distinct components of the EGC current system are labeled at the top of the velocity sections in Figures 2–4 and will be discussed separately in the following sections.

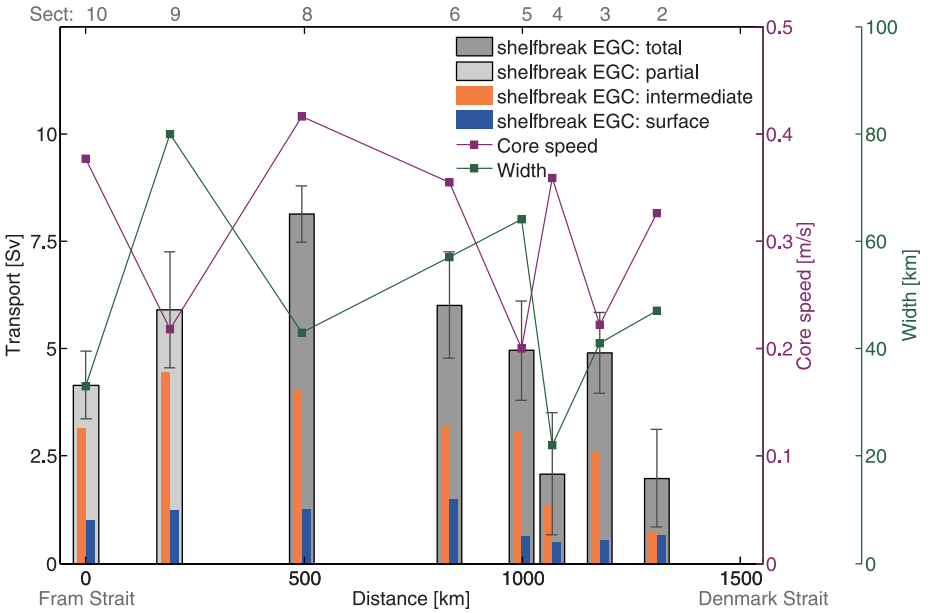

Figure 6. Volume transport of the shelfbreak EGC at each of the sections. The dark gray bars represent the volume transport where the entire branch was sampled and for sections 9 and 10 the light gray bars indicate that only the upper 800 m was measured. The orange and blue bars show the transport of intermediate and surface layers, respectively. Also shown are the core speed (purple line) and the width (green line) of the shelfbreak EGC. The *x* axis indicates the along-stream distance from Fram Strait to Denmark Strait.

4.1. The Shelfbreak EGC

The shelfbreak EGC was the most prominent component of the boundary current system. It was characterized by strong surface-intensified flow close to the shelfbreak with a depth-dependent deep extension. The center of the current was objectively identified as the location with the highest mean absolute geostrophic velocity over the top 150 m across the section. In all cases, this was associated with a density front, characterized by a steep shoaling of the 27.5 kg/m^3 isopycnal. It also generally corresponded to the hydrographic front between the PSW and the Atlantic-origin Water. The bounding limits of the shelfbreak EGC were typically chosen as the locations where the mean velocity over the upper 150 m was reduced to 20% of the core value. This worked as a guideline, but in several instances, we subjectively chose the boundaries by combining the characteristic hydrography of the shelfbreak EGC and the steep slope of the 27.5 kg/m^3 isopycnal toward the east. The resulting borders of the current are marked by the black vertical lines in the velocity sections of Figures 2–4.

The width and strength of the shelfbreak EGC varied considerably from section to section (Figure 6). The core speed ranged between 0.2 and 0.4 m/s but showed no clear trend from north to south. The width of the current varied from a maximum value of 80 km at section 9 to only 22 km at section 4, with indication of an overall decrease as the current progressed from Fram Strait to Denmark Strait. For the most part, the width and the strength varied out of phase with each other: a strong current core coincided with a narrow jet and vice versa.

4.2. The Polar Surface Water Jet

At each of the transects that sampled close to the east Greenland coast, a surface-intensified jet was present within the PSW layer, onshore of—and distinct from—the shelfbreak EGC. This PSW Jet was completely bracketed on sections 6, 3, and 2, and partly sampled on sections 8 and 4 (the latter two sections did not extend sufficiently far onshore to fully sample the feature). The jet carried mostly PSW, but a weak extension to the bottom also resulted in transport of some Atlantic-origin Water that had penetrated onto the shelf. The velocity of the current was slightly lower than the shelfbreak EGC, with a peak value close to 0.2 m/s in section 3 (the core was defined in similar fashion to the shelfbreak EGC). Due to the low salinity of the PSW, this branch of the current system is very important for the freshwater transport (discussed below in section 5.2).

South of Denmark Strait, the East Greenland Coastal Current (EGCC) is a well-established feature [*Bacon et al.*, 2002; *Sutherland and Pickart*, 2008]. The PSW Jet shares some similarities with this current, such as the proximity to the coast and its hydrographic structure, although the velocities within the PSW Jet were

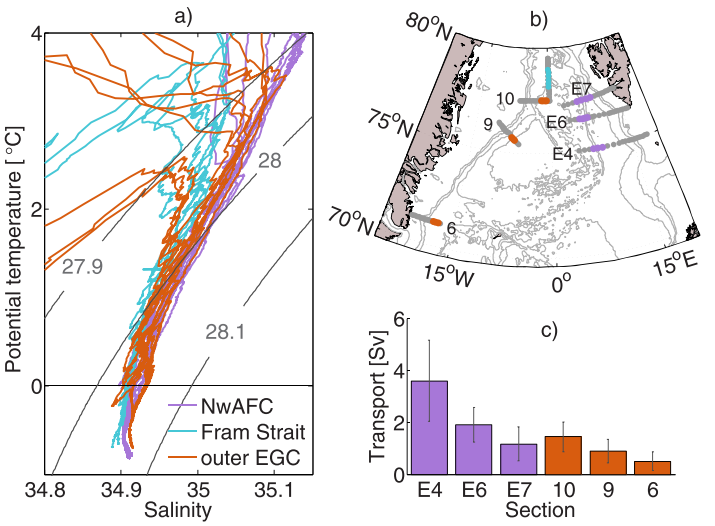

Figure 7. (a) Potential temperature/salinity diagram of the stations in the NwAFC/western branch of the WSC and the outer EGC, where the stations from the meridional section (named Fram Strait) are represented by the profiles from 2003. The three stations in orange with a temperature maximum just above 2°C are from section 6. (b) Map of the sections where these branches of the current system were detected, with the stations shown in Figure 7a highlighted in colors. (c) Transport of Atlantic-origin Water in this part of the current system, where positive transport is in the along-stream direction.

generally weaker than those of the EGCC [*Sutherland and Pickart*, 2008]. The volume transports of the PSW Jet in the sections that fully resolved it were in the range of 0.54 ± 0.28 to 0.83 ± 0.27 Sv. These transports are comparable to the values obtained by *Sutherland and Pickart* [2008] for the EGCC, ranging from 0.6 to 1.4 Sv, as well as the estimate by *Bacon et al.* [2002] of 1 Sv. *Bacon et al.* [2008] suggested that the EGCC could also be present north of Denmark Strait. They calculated the volume transport of the coastal current observed by *Nilsson et al.* [2008] close to 72°N to be 0.77 Sv.

Bacon et al. [2002] described the formation of the EGCC as a result of meltwater runoff from Greenland leading to a strengthening of the cross-shelf salinity gradient. This process is likely seasonal, with strongest current velocities in summer when the amount of meltwater is largest. By contrast, *Sutherland and Pickart* [2008] suggested that the EGCC is formed by a bifurcation of the shelfbreak EGC south of Denmark Strait due to bathymetric steering by the Kangerdlugssuaq Trough. If the EGCC is in fact the result of branching of the EGC south of Denmark Strait, then the PSW Jet is obviously not the same feature as the EGCC. On the other hand, if the EGCC stems from meltwater runoff as proposed by *Bacon et al.* [2002] then there is no geographical reason why it cannot also be present north of Denmark Strait. However, the presence of a coastal current during spring presented in *Nilsson et al.* [2008] shows that this feature is not restricted to summer. At present it remains unclear whether the PSW Jet is connected to the EGCC and what mechanism is responsible for generating this branch.

4.3. The Outer EGC

Offshore of the shelfbreak EGC, at sections 6, 9, and 10, we observed a distinct branch advecting Atlantic-origin Water equatorward (see bottom of Figures 2 and 3). As is the case with the shelfbreak EGC, this outer branch of the EGC is associated with a density front (i.e., shoaling isopycnals offshore), although the baroclinic shear is weaker. At section 8, this current branch was not observed and the current velocities offshore of the shelfbreak current were weak (Figure 5). This could be the result of a meandering of this outer branch offshore of our section or synoptic variability masking its presence. Using data from a yearlong deployment of moorings in the EGC, stretching from the slope toward the interior Greenland Sea at 75°N, *Woodgate et al.* [1999] found that the current had two independent cores: one at the shelfbreak and one above the base of the continental slope. This was not a persistent feature in their time series, and at times the two cores appeared to merge.

In order to investigate the relationship of the outer EGC to the boundary current system in the eastern Nordic Seas—specifically to the Atlantic Water approaching Fram Strait—we considered sections E7, E6, and E4 from the IOPAN survey (see Figures 1 and 7b for the IOPAN section locations). In the eastern sections, an analogous offshore current core, seaward of the eastern WSC, was present (not shown). This is the western branch of the WSC which constitutes the northward extension of the Norwegian Atlantic Frontal Current (NwAFC) [*Orvik and Niiler*, 2002; *Walczowski*, 2013]. The western branch advects Atlantic Water toward Fram Strait along the slope of the Knipovich Ridge (Figure 1). To investigate a possible link between the two outer current cores, we constructed a composite summer section along the 0°E meridian in Fram Strait using the historical CTD data described in section 2.2 (Figures 1 and 7b). The composite section reveals the presence

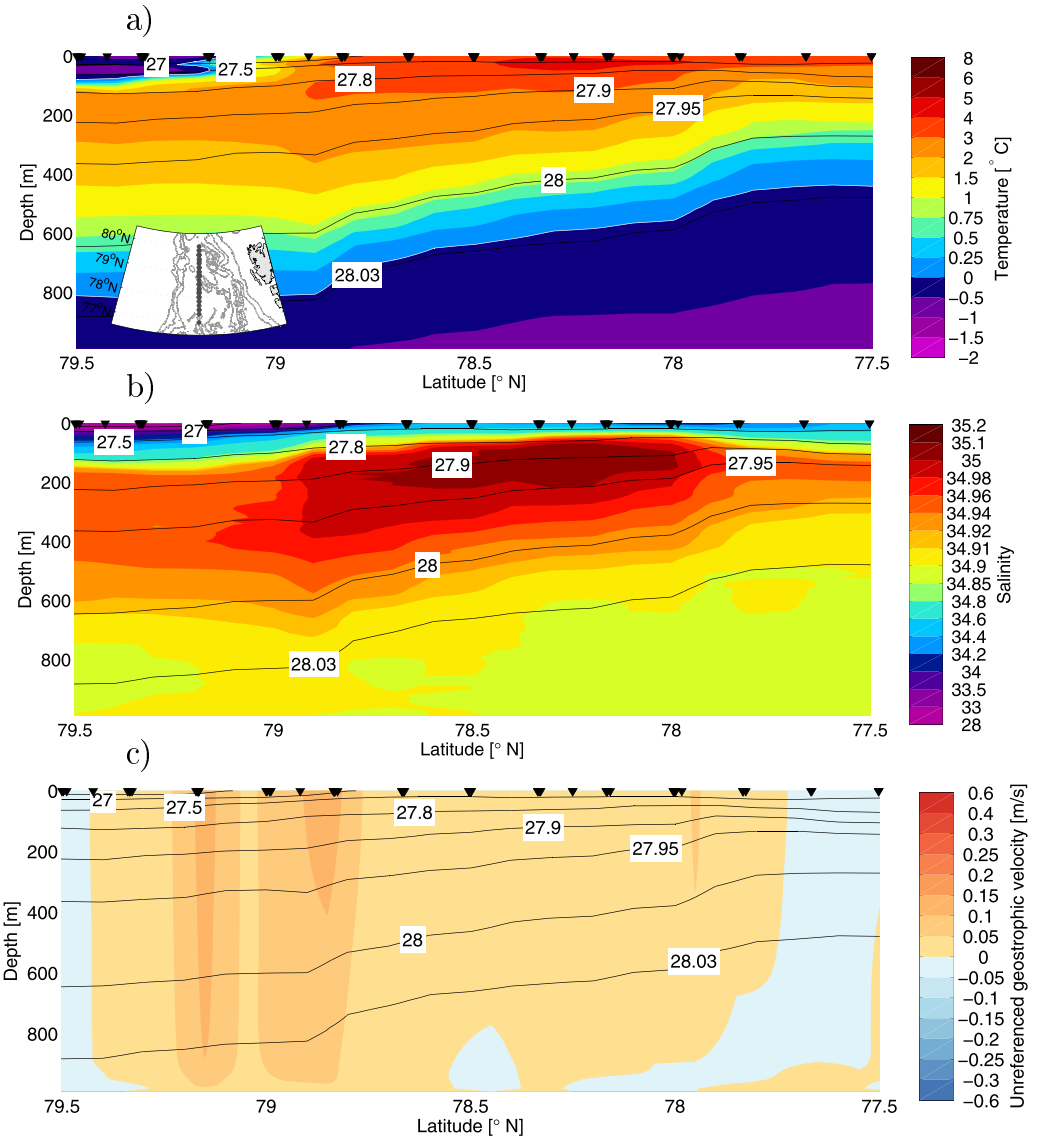

Figure 8. Mean meridional (close to 0°E) vertical section of (a) potential temperature, (b) salinity, and (c) geostrophic velocity relative to a level of no motion at 1000 m, based on Fram Strait summer sections from the years 1997–1999 and 2002–2004. The inset shows the location of the section. Positive flow is toward the west. The white contours in Figure 8a are the 0°C isotherms and the black contours are isopycnals (kg/m^3). The black inverted triangles along the top indicate the locations of the 75 stations contributing to the mean.

of a core of warm and saline Atlantic-origin Water located between 78°N and 79°N (Figures 8a and 8b). Notably, the hydrographic properties of the Atlantic Water flowing northward toward Fram Strait in the western WSC closely match both the warm and salty water in the composite section as well as the Atlantic-origin Water flowing southward in the outer core of the EGC (Figure 7a, where for clarity we show only the profiles from 2003 in Fram Strait). This suggests that the outer core of the EGC is the continuation of the western branch of the WSC, in accordance with the notion of a direct recirculation of Atlantic Water in Fram Strait north of sections E7 and 10 [e.g., *Quadfasel et al*., 1987; *Manley*, 1995; *Fahrbach et al*., 2001; *Marnela et al*., 2013].

Unfortunately, there are no corresponding velocity data to the historical hydrographic data, but the baroclinic shear relative to 1000 m is consistent with a region of surface-intensified westward flow associated with the hydrographic front on the northern side of the warm, salty core (Figure 8c). This provides further evidence that the western branch of the WSC retroflects in Fram Strait and that this is the outer branch of the EGC that we sample farther downstream. Progressing along this recirculating branch, the transport of

Atlantic-origin Water steadily decreases (Figure 7c). Note that the transports were estimated perpendicular to the sections, hence, the actual transport might be larger depending on the direction of the flow. We have made no attempt to estimate the transport across the composite meridional section because of the lack of direct velocity information there. There is a particularly large drop in transport of the western branch of the WSC from section E4 to section E6, which may be influenced by a couple of factors. First, *Walczowski and Piechura* [2007] found that parts of the NwAFC are diverted offshore well south of Fram Strait. While their data suggest that this happens south of section E4, it could be a spatially or temporally varying process and our results may be a reflection of this. Second, a mesoscale eddy was located at the offshore end of section E4 which made it difficult to precisely estimate the transport of the western branch at that location; this is reflected by the large error bar corresponding to the E4 transport value (Figure 7c). Nonetheless it is clear that, despite the synoptic nature of the two shipboard surveys, there is a systematic decrease in transport of the outer core of Atlantic-origin Water as it flows along the perimeter of the Nordic Seas toward Denmark Strait.

The notion of a direct recirculation across Fram Strait has been discussed in a number of previous studies, and this flow is referred to as the Return Atlantic Current [e.g., *Paquette et al*., 1985; *Quadfasel et al*., 1987]. *Manley* [1995] found that the recirculation took place south of 79°N. *Bourke et al*. [1988] estimated the transport from continuity to be 0.8 Sv, which is lower than our value of 1.6 Sv in section 10. Also, based on conservation constraints, *Marnela et al*. [2013] estimated the recirculation of Atlantic Water to be about 2 Sv. A mooring array has monitored the flow through Fram Strait since 1997 [e.g., *de Steur et al*., 2009; *Beszczynska-Möller et al*., 2012]. In 2002, the moorings in the western part of the strait were moved from 79°N to 78°50′N, resulting in an increase in the volume transport of the EGC of about 3 Sv. This suggests that a recirculation of Atlantic-origin Water of this magnitude takes place south of 79°N [*de Steur et al*., 2014]. It should be noted that this is the total change in the volume transport of the EGC, and not directly comparable to the recirculation resulting in the outer EGC. Using a high-resolution numerical model, *Aksenov et al*. [2010] referred to the recirculation in Fram Strait as the Knipovich Branch, and calculated a volume transport of 1.2 Sv. This was supported by *Hattermann et al*. [2016], who found a similar recirculation in the southern Fram Strait which they linked to the cyclonic gyre circulation in the Greenland Sea. However, our measurements indicate that the outer EGC branch is also present south of the Greenland Sea gyre (section 6). In the early studies that first introduced the term Return Atlantic Current, it was depicted as a flow that merged with the shelfbreak EGC beneath the PSW layer. We have shown instead that these two features exist side-by-side in the Greenland Sea, at least as far south as the Jan Mayen Fracture Zone.

4.4. The Separated EGC and Eddies in the Blosseville Basin

The separated branch of the EGC in the Blosseville Basin, first identified by *Våge et al*. [2013], was evident in sections 2 and 3 (we note that *Våge et al*. [2013] included section 2 in their study). In section 3, this branch was situated close to $x = 165$ km, identifiable as a distinct surface-intensified current with a deep extension to the bottom (Figure 4c). This coincided with the hydrographic front between the PSW and the ambient water (Figures 4a and 4b). *Våge et al*. [2013] proposed two possible mechanisms for the formation of the separated EGC. First, they demonstrated that the orography of Greenland, in combination with the predominantly northerly barrier winds [*Harden et al*., 2011], results in negative wind stress curl across the Blosseville Basin. It was hypothesized that this, in combination with the closed isobaths of the basin, could spin up an anticyclonic gyre whose offshore branch is the separated EGC. The moored measurements of *Harden et al*. [2016] are consistent with this notion. The second hypothesis of *Våge et al*. [2013] for the formation of the separated EGC, based on idealized numerical simulations, is that baroclinic instability of the shelfbreak EGC at the northern end of the Blosseville Basin generates anticyclonic eddies that migrate offshore and coalesce as they encounter the base of the Iceland slope. In the model, this merging of eddies forms the offshore branch of the current.

In the southern part of our domain, in sections 2–5, both cyclonic and anticyclonic eddies were observed. The anticyclones typically had a core of Atlantic-origin Water, whereas the cyclones had a core of ambient water. The eddies were likely formed via baroclinic instability of the shelfbreak EGC. This process should form dipole pairs: the anticyclone associated with the meandering of the current, and the weaker near-field cyclone adjacent to the meander. The latter features are displaced deeper in the water column and tend to wrap boundary current water around their edges [e.g., *Spall*, 1995]. While eddies of both signs are formed

initially (and are necessary for self-advection offshore), the cyclones tend to spin down more readily so that, in the far field, anticyclones typically dominate [*Lilly et al*., 2003].

In section 3, we sampled a 30 km diameter cyclone close to the offshore edge of the shelfbreak EGC, centered near x = 100 km where relatively cool and fresh ambient water interrupted the Atlantic-origin Water otherwise present in this part of the section (Figures 4a and 4b). Note the pinching of isopycnals near 100 m depth (e.g., the 27.8 and 27.95 kg/m^3 density contours), consistent with the subsurface maximum in velocity of this feature, versus the surface-intensified core of the shelfbreak EGC. The lateral boundary between the eddy and the boundary current was determined by balancing mass in the cyclone. *Våge et al*. [2013] identified a critical region north of Denmark Strait for the shedding of eddies from the shelfbreak EGC associated with the formation of the separated EGC. In their numerical simulations, the eddies originated from the continental slope at the northern end of the Blosseville Basin near 69°N where there is a pronounced curvature in the bathymetry (Figure 1). The eddies that were sampled on sections 2–5 are generally consistent with this idea that the separated EGC is formed by eddies coalescing along the base of the Iceland slope.

5. Transports

Our estimates of volume transport depend on the strength of the current as well as our semiobjective choice of the lateral bounds of the feature in question and how well it is sampled. Of the different components identified in the EGC system, the shelfbreak branch was the most important in terms of volume transport and also the best sampled. As such, we focus on the along-stream evolution of the volume transport of this part of the boundary current system.

5.1. Volume Transport of the Shelfbreak EGC

The large section-to-section variability in core speed and width of the shelfbreak EGC noted earlier (Figure 6) indicates that the current is very dynamic. However, these two aspects tend to offset each other to some degree, resulting in a more interpretable signal in volume transport. The current had a significant barotropic component and hence to estimate the total transport, measurements to the bottom would be required. Unfortunately this was not achieved in the two northernmost sections where the CTD casts extended only to 800 m depth (due to time constraints). In light of the fact that the bottom depth at some of the stations on these sections exceeded 3000 m, the total transports in sections 9 and 10 are clearly underestimates. Even so, we include the partial estimates for completeness.

Taking into account the underestimated transports in the northern sections, it is evident that the total transport of the shelfbreak EGC decreased from north to south, with variability about this trend (Figure 6). Such a decrease is to be expected, since water is diverted from the boundary between Fram Strait and Denmark Strait (e.g., via the Jan Mayen Current [*Bourke et al*., 1992], the East Icelandic Current [*Macrander et al*., 2014], and the bifurcation of the EGC in the Blosseville Basin). When calculating the mean volume transport of the EGC using mooring data from the Greenland Sea, *Woodgate et al*. [1999] divided the transport estimates into a throughput and a recirculation according to whether the temperature was above or below 0°C, respectively. The annual mean throughput estimated by *Woodgate et al*. [1999] was 8 ± 1 Sv, which can be compared to our value of the transport above the lower 0°C isotherm at sections 8 and 9 in the Greenland Sea of 5.3 ± 1.4 and 5.7 ± 0.95 Sv, respectively. Our estimates are lower than theirs, but within the short-term variability exhibited in their time series. (The difference is not due to a sampling issue since the lower 0°C isotherm was above 800 m in section 9.)

We apply the throughput definition of *Woodgate et al*. [1999] outside the Greenland Sea as well as a means to isolate the part of the shelfbreak EGC that exits the Nordic Seas through Denmark Strait. Although the depth of the lower 0°C isotherm is generally deeper than the sill depth of Denmark Strait (650 m), *Harden et al*. [2016] recently demonstrated that a portion of the overflow water aspirates from depths greater than this. As shown below, the choice of the 0°C isotherm appears to be realistic. We further partition the shelfbreak EGC transport into a surface layer contribution and an intermediate layer contribution, where the surface layer extends to the 27.7 kg/m^3 isopycnal and the intermediate layer extends from there to the deep 0°C isotherm (as described in section 3). This reveals that there are different trends in the two different parts of the water column.

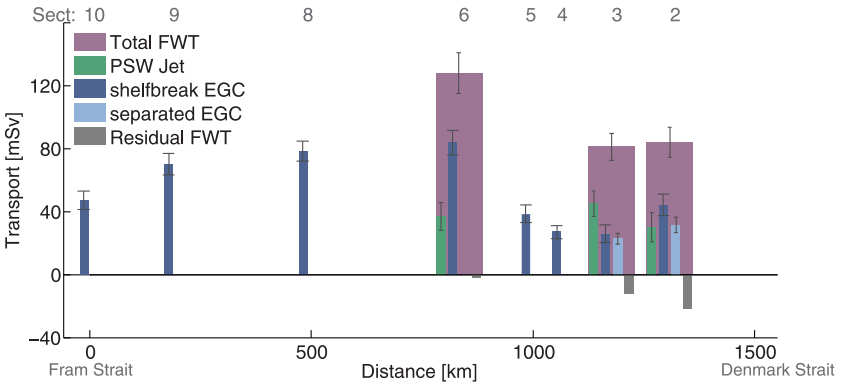

Figure 9. Freshwater transports in the different branches of the EGC system (PSW Jet in green, the shelfbreak EGC in dark blue, and the separated EGC in light blue), using a reference salinity of 34.8 (see equation (1)). The purple bars show the total FWT for those sections covering the entire shelf. The residual transport (gray bars) is the transport outside the defined branches. The *x* axis indicates the along-stream distance from Fram Strait to Denmark Strait.

As seen in Figure 6, the transport of surface water (which is completely captured in all of our sections) was more or less constant among the four northernmost sections at approximately 1.2 ± 0.1 Sv, with a lower mean value around 0.6 ± 0.1 Sv for the sections to the south. An offshore transport of surface waters in this area is supported both by observations, showing relatively fresh waters offshore of the shelfbreak in and north of the Blosseville Basin, and by idealized numerical modeling showing eddies carrying near-surface EGC water offshore [*Våge et al*., 2013]. By contrast, the transport of the intermediate water decreased steadily from north to south, with sections 4 and 2 having particularly low values (Figure 6). This was a result of a very narrow current in section 4 (not adequately compensated for by the strong velocity) and a region of northward velocities within the shelfbreak part of the current in section 2. This highlights the inherent variability in a synoptic survey; indeed, mooring-based studies of the EGC [e.g., *Woodgate et al*., 1999; *Harden et al*., 2016] have indicated that individual realizations can differ significantly from long-term means.

The dense overflow water flowing through Denmark Strait is traditionally defined as having a density greater than $\sigma_\theta = 27.8$ kg/m^3 [*Dickson and Brown*, 1994], and previous transport estimates in the Iceland Sea [e.g., *Våge et al*., 2011, 2013] have used the sill depth as the lower limit. Here we take the intermediate layer defined above as an approximate representation of the overflow water (noting that the difference in depth of the 27.7 and 27.8 kg/m^3 isopycnals in each of our sections is small). This results in a mean overflow water transport of 2.8 ± 0.7 Sv, which is close to the annual mean value of 2.54 ± 0.16 Sv obtained by *Harden et al*. [2016] at the location of section 2. This good agreement supports our choice of the deep 0°C isotherm as the lower limit for the overflow water, and also suggests that any aspiration below this level is limited.

5.2. Freshwater Transport

Most of the freshwater sampled during the survey resided on the east Greenland shelf and in the shelfbreak EGC. Recall that only sections 2, 3, and 6 covered the entire shelf/EGC system (Figure 1), so for the other sections, the FWT was calculated only for the shelfbreak EGC. While the 34.8 isohaline shoaled to the east along each section, it only outcropped at the seaward end of section 9 (last station) and on section 10; hence, some portion of the FWT relative to this isohaline occurred outside most of the sections. The total calculated FWT ranged from a maximum of 127 ± 13 mSv at section 6 to a minimum of 81 ± 8 mSv at section 3 (Figure 9). The FWT of the shelfbreak EGC, calculated for every section, revealed the same pattern as the volume transport of the surface layer with a clear decrease south of the Jan Mayen Fracture Zone. In the sections extending onto the shelf, the FWT in the PSW Jet ranged between 29% of the total FWT (section 2) and 55% (section 3). Due to the very low presence of freshwater in the outer EGC, the contribution from this branch was less than 5 mSv in sections 6 and 9, and close to 0 in section 10 (not plotted in Figure 9). In the two southernmost sections where the separated EGC was present, it contributed 25% and 37% to the total FWT, emphasizing the importance of the bifurcation in diverting freshwater into the interior. This partitioning of the FWT into the different branches of the EGC highlights the importance of sampling the entire width of the current system, in particular the full width of the shelf as the PSW Jet is responsible for a sizeable fraction of the FWT.

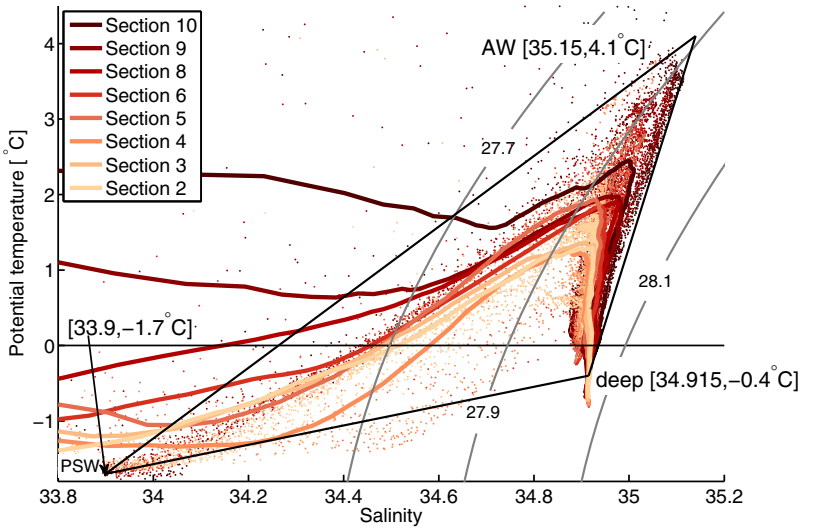

Figure 10. Potential temperature/salinity diagram of all profiles from the EGC survey where Atlantic-origin Water was present. The dots are individual measurements and the solid lines represent the mean profile from each section. The end-members discussed in the text are indicated by the corners of the triangle. AW is Atlantic Water.

We compare our FWT estimates from section 2 and 3 to previous results based on observations obtained along our section 2. All estimates are relative to a reference salinity of 34.8. *Våge et al*. [2013] calculated the FWT from four high-resolution transects obtained along this section. They divided the FWT between the shelfbreak branch and the separated branch. The two branches contributed 108 ± 24 and 29 ± 7 mSv, respectively. Their mean FWT in the shelfbreak branch was higher than ours, both as a result of synoptic variability and due to the fact that they did not consider the PSW Jet a distinct branch. However, the relative contribution of the separated branch to the total FWT (25%) was similar to our estimate (31%).

The East Icelandic Current separates from the EGC between section 6 and the Blosseville Basin. Recently *Macrander et al*. [2014] estimated the mean FWT in this current from a decade of observations at the Langanes section northeast of Iceland to be 3.4 ± 0.3 mSv (relative to a salinity of 34.93). This is an order of magnitude lower than the approximate 50 mSv reduction in FWT from section 6 to the Blosseville Basin calculated in our survey, suggesting that if the East Icelandic Current contributes to this reduction it would have to lose most of its FWT before reaching Langanes. (The discrepancy is not sensitive to the choice of reference salinity.) The mesoscale eddy activity south of the Jan Mayen Fracture Zone could transport freshwater off the boundary and contribute to a freshening of the western Iceland Sea, between the Kolbeinsey Ridge and the Greenland shelf. We assume that the observed eddies are symmetric and as long as we cover their entire width, our estimates of the total FWT is not susceptible to their presence. Also, we did not sample eddies on the offshore ends of the sections. We will return to the fate of the FWT diverted offshore in section 7.

6. Along-Stream Water Mass Modification

Thus far, we have discussed water masses in terms of the three-layered structure introduced in section 3: PSW, Atlantic-origin Water, and the lower intermediate layer. Previous studies [e.g., *Rudels et al*., 2002, 2005; *Jeansson et al*., 2008] have presented details of the water masses of the EGC system and how they are modified from Fram Strait to Denmark Strait. We do not attempt the same detailed analysis here, but rather focus on the along-stream modification of the Atlantic-origin Water, which has potential implications for the dense overflow water passing through Denmark Strait.

6.1. Modification of the Atlantic-Origin Water

All of the CTD profiles in the survey with a temperature maximum above 0°C below the 27.7 kg/m^3 isopycnal contained Atlantic-origin Water. These are shown in Figure 10 in the θ/S plane and are color coded according to their section number. We also computed a single average profile for each section and these are included in Figure 10 as solid lines. Section 10 is unique in that there is a large amount of Atlantic-origin

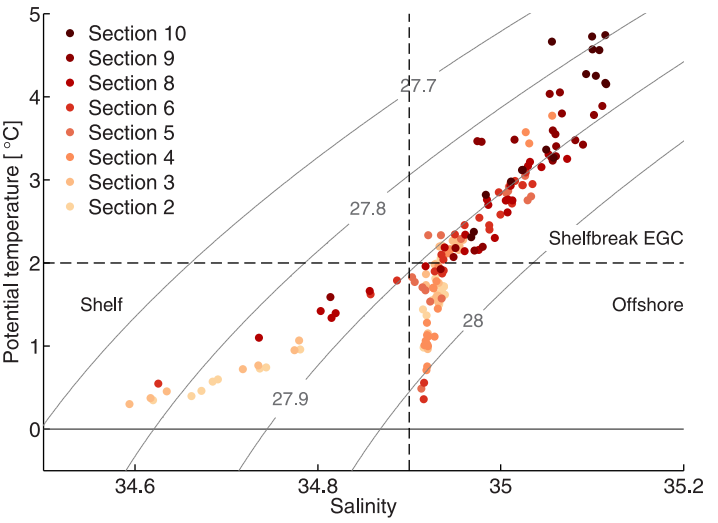

Figure 11. Potential temperature/salinity values corresponding to the core of the Atlantic-origin Water for the stations of the EGC survey. The horizontal dashed line is the 2°C isotherm and the vertical dashed line is the 34.9 isohaline. The quadrants discussed in the text correspond to the shelfbreak EGC (also containing some offshore stations), the offshore water, and the water on the shelf.

Water extending to the offshore end of the section, and, notably, this water mass was in direct contact with the atmosphere. By contrast, farther south a thin layer of PSW extended over most of each of the transects (compare Figures 2 and 3). Combined with the fact that the Atlantic-origin Water generally becomes colder and less saline enroute from Fram Strait to Denmark Strait (Figures 2–4), this means that, in the northern part of the domain, the average θ/S profiles are substantially warmer in the upper part of the water column (Figure 10). This is most extreme at section 10 in Fram Strait.

We now focus on the alongstream change in hydrographic properties of the core of the Atlantic-origin Water, which allows us to assess the mixing that has taken place. For each CTD profile, the core of the Atlantic-origin Water was identified by the intermediate temperature maximum. Figure 11 shows the θ/S properties of the core for the entire survey. In the quadrant marked "shelfbreak EGC," the properties of the core were predominantly modified isopycnally (approximately along the 27.9 kg/m^3 isopycnal). The largest deviation from this was found in some of the offshore profiles on section 10 where the core density was closer to 27.8 kg/m^3. Recall that the Atlantic-origin Water, there was still in contact with the atmosphere; an additional cooling of 0.5–1°C would modify the water enough to reach the 27.9 kg/m^3 density level. In the quadrant marked "offshore", the Atlantic-origin Water seaward of the shelfbreak EGC was undergoing diapycnal mixing resulting in a change in temperature but only small changes in salinity. Finally, the "shelf" quadrant shows a tail toward low salinities corresponding to stations on the east Greenland shelf in sections 6, 3, and 2 that are strongly modified by the fresh PSW. We note that all the stations in the shelfbreak current are found in the quadrant marked "Shelfbreak EGC," plus some offshore stations which contain relatively unmodified Atlantic-origin Water (see e.g., Figure 2 where the warm Atlantic-origin Water had spread well east of the shelfbreak current.) In the other two quadrants, the water is solely from the indicated region. We will consider in more detail the modification of the Atlantic-origin Water within and offshore of the shelfbreak EGC separately in sections 6.1.1 and 6.1.2.

What water masses mixed with the Atlantic-origin Water in order to change its core properties as depicted in Figure 11? The θ/S diagram in Figure 10 illustrates the end-member water masses available for mixing. By drawing a mixing triangle it appears that nearly all of the hydrographic measurements can be represented by a combination of PSW, Atlantic Water, and a deep water mass. We note that this definition of the deep water mass is within historical definitions of intermediate waters such as the upper Polar Deep Water and Arctic Intermediate Water [*Rudels et al.*, 2005]; in the present context, deep water refers to water denser than the Atlantic-origin Water. From these three end-members, we calculated their relative contributions to the Atlantic-origin core for each profile. The resulting percentages of each end-member showed large variability from station to station across the sections (Figure 12), consistent with the variable core properties described above. PSW typically contributed around 10%, with the exception of some locations on the shelf where it was more prominent (these also constitute the low salinity tail in Figure 11). The deep water contribution became increasingly important toward the south, and the Atlantic Water fraction, which dominated in the north, was reduced to around 50% in sections 2 and 3 (the PSW percentage was larger at the shoreward ends of these two sections). In sections 2–6, the region offshore of the shelfbreak EGC contained a larger fraction of deep water.

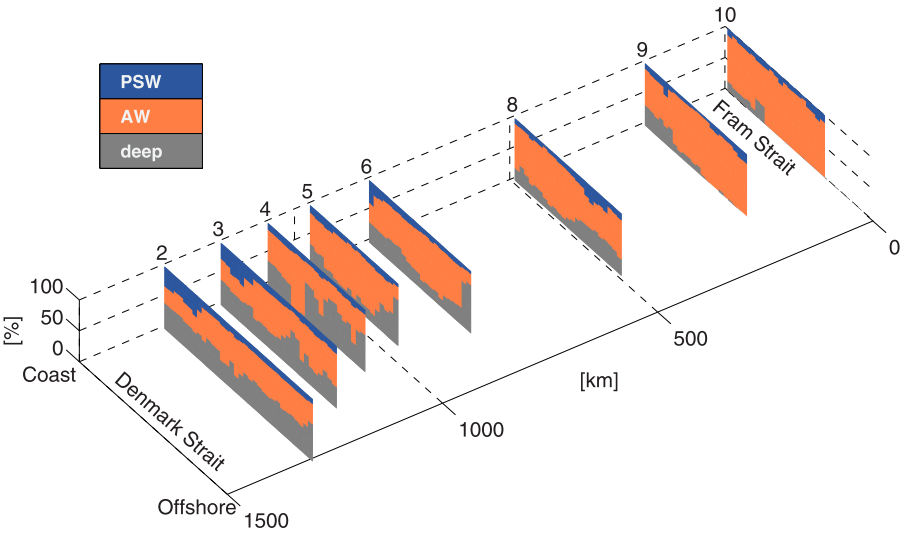

Figure 12. Percent contribution of the water mass end-members in Figure 10 to the core properties of the Atlantic-origin Water. The sections are labeled on top of the *z* axis and plotted relative to their along-stream distance from Fram Strait.

6.1.1. Atlantic-Origin Water Within the Shelfbreak EGC

All of the Atlantic-origin core values within the shelfbreak EGC were characterized by a core temperature above 2°C (all eight sections were represented in this quadrant). In addition, some of the profiles offshore of the shelfbreak current were characterized by the same relatively high temperature. Since the core properties of these profiles change in the same manner as those in the shelfbreak region, we focus the discussion on the stations within the shelfbreak current. In general, this water cooled and freshened isopycnally as it progressed southward. However, core values as far south as section 4 had similar properties to the Atlantic Water sampled in Fram Strait (Figure 11), demonstrating that some Atlantic Water can be advected with little modification from Fram Strait all the way to Blosseville Basin. This variability in the degree of along-stream isopycnal modification within the shelfbreak EGC could be due to sporadic mixing with the colder and fresher ambient waters stemming from the interior of the Greenland and Iceland Seas.

In order to explore this possibility, we constructed average profiles of temperature and salinity from each of the two seas using the historical database described in *Våge et al*. [2013] (not shown). By comparing the typical hydrographic properties at the 27.9 kg/m^3 isopycnal in the interior seas ($\theta = 0.7$°C, S = 34.8 in the Iceland Sea and $\theta = 1.2$°C, S = 34.8 in the Greenland Sea) with the corresponding values in the shelfbreak EGC, the potential for isopycnal modification of the Atlantic-origin Water was evaluated. We found it unlikely that these interior waters influence the shelfbreak EGC (or even the offshore Atlantic-origin Water), for several reasons. This includes the fact that there is a significant mismatch in the hydrographic properties at the 27.9 kg/m^3 isopycnal between the boundary current and the interior basins, and the fact that the 27.9 kg/m^3 isopycnal outcrops quite far from the center of the basins over a large part of the year, hence preventing such an exchange. As an example, most of the Atlantic-origin Water within the shelfbreak current from section 5 and southward would need an addition of more than 50% Iceland Sea water to obtain the observed core hydrographic properties. The Iceland Sea water mass is barely present in any of the casts on our sections, suggesting that it is not readily available for mixing with the Atlantic-origin Water in the core of the shelfbreak EGC. Similar mixing ratios are found in the Greenland Sea, though with larger variability from cast to cast.

In light of the end-member calculation above, it seems more likely that the PSW and deep water mix with the Atlantic-origin Water in the shelfbreak EGC and modify it isopycnally as it progresses from Fram Strait to Denmark Strait. Notably, such modification along density surfaces supports the view, first proposed by *Mauritzen* [1996], that the Atlantic-origin Water is mostly densified in the eastern part of the Nordic Seas via air-sea fluxes.

6.1.2. Atlantic-Origin Water Offshore of the Shelfbreak EGC

In the sections south of the Jan Mayen Fracture Zone (sections 2–6), the Atlantic-origin Water offshore of the shelfbreak EGC was modified diapycnally (lower right quadrant of Figure 11). This was likely due to

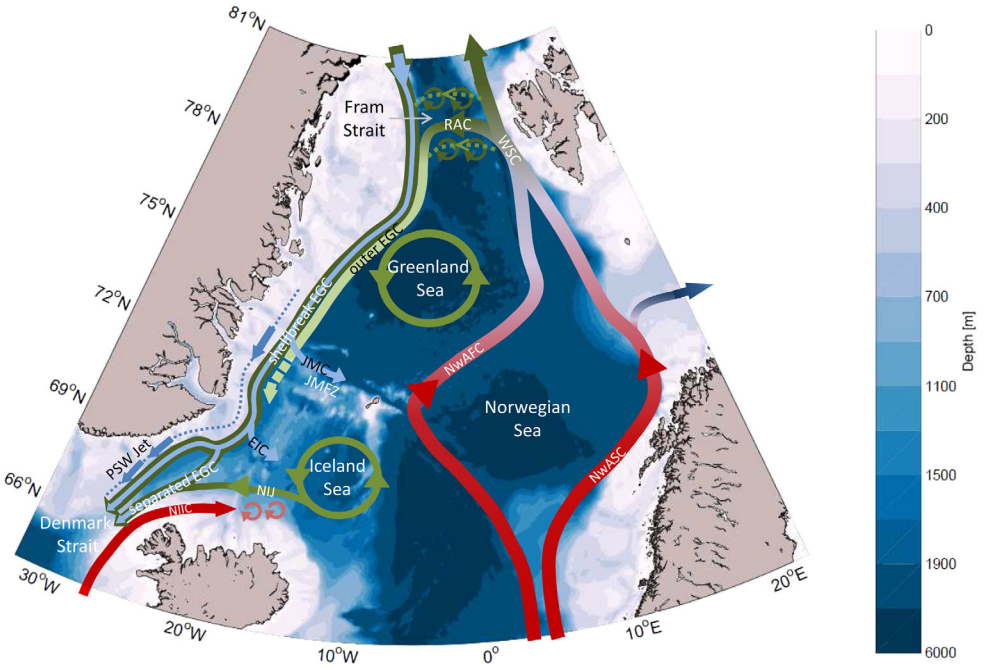

Figure 13. Schematic circulation of warm Atlantic Water in the Nordic Seas. Its transformation to colder, fresher, and denser Atlantic-origin Water in the rim current of the Nordic Seas and Arctic Ocean is illustrated with a transition from red to green colors. The fresh PSW in the EGC is indicated in blue. The green circles in the Greenland and Iceland Seas indicate cyclonic gyres. The acronyms are: NwASC = Norwegian Atlantic Slope Current; NwAFC = Norwegian Atlantic Frontal Current; WSC = West Spitsbergen Current; RAC = Return Atlantic Current; JMC = Jan Mayen Current; JMFZ = Jan Mayen Fracture Zone; NIJ = North Icelandic Jet; EIC = East Icelandic Current; and NIIC = North Icelandic Irminger Current.

mixing with the deep water, considering the relatively high percentage of that water mass in these sections (Figure 12). Interestingly, the offshore Atlantic-origin Water salinity appeared to reach a threshold value, marked by the 34.9 isohaline in Figure 11. The depth of the temperature maximum in the Atlantic-origin Water was shallower offshore than within the shelfbreak EGC, even though the density was higher. This was due to the strong stratification in the top 50 m. Below that the intermediate salinity maximum, characteristic of the shelfbreak EGC, was largely eroded.

7. Discussion and Conclusions

A high-resolution hydrographic/velocity survey of the East Greenland Current (EGC), conducted in summer 2012, revealed that the current had three distinct branches: the shelfbreak EGC situated in the vicinity of the shelfbreak, the Polar Surface Water (PSW) Jet on the continental shelf, and the outer EGC over the mid to deep continental slope. In Figure 13, we provide a schematic overview of the circulation in the Nordic Seas that includes these branches and their presumed upstream sources. Atlantic Water enters the Nordic Seas in the southeast both via the Iceland-Faroe and the Faroe-Shetland inflows [*Hansen et al*., 2015]. Farther north, this leads to two distinct branches that transport Atlantic Water poleward: the Norwegian Atlantic Slope Current (NwASC) following the continental shelfbreak offshore of Norway and the Norwegian Atlantic Frontal Current (NwAFC) situated at the hydrographic front between the Atlantic Water in the Norwegian Sea and the colder and fresher water in the Greenland Sea [*Orvik and Niiler*, 2002]. In Fram Strait, the two branches appear to continue along different trajectories. The NwASC progresses northward toward the Arctic Ocean in the eastern branch of the WSC [*Beszczynska-Möller et al*., 2012], whereas the NwAFC constitutes the western branch of the WSC which recirculates in Fram Strait and forms the outer EGC. This recirculation provides a direct pathway for Atlantic Water across Fram Strait. Previous studies have shown that Atlantic Water is also fluxed westward in the northern part of Fram Strait by extensive eddy activity, subsequently merging with the shelfbreak EGC [*von Appen et al*., 2016; *Hattermann et al*., 2016].

The outer EGC and the shelfbreak EGC flow equatorward side-by-side at least as far south as the Jan Mayen Fracture Zone. Along this pathway, the volume transport of the outer EGC decreases. This gradual

disintegration might be a result of baroclinic instability, similar to what is believed to take place in the western Arctic boundary current [*von Appen and Pickart*, 2012]. On the other hand, our sampling could be biased due to temporal variability. In the Blosseville Basin, the separated EGC is associated with a similar baroclinic front as the outer EGC, and they could potentially be connected. However, this is not evident from our survey. Also, the separated EGC carries an order of magnitude more freshwater than the outer EGC. At sections 9 and 10, the outer EGC was directed along the shelf break, whereas a more southeastward direction was observed at section 6 (Figure 5). This could indicate an offshore veering of the current toward the Iceland Sea south of section 6. In summary, the fate of the outer EGC south of the Jan Mayen Fracture Zone is not clear and it remains an open question as to whether it disintegrates, continues equatorward toward Denmark Strait, or is diverted into the Iceland Sea.

A portion of the surface water in the shelfbreak EGC is fluxed offshore in the Jan Mayen and East Icelandic Currents (Figure 13). In the northern end of the Blosseville Basin, the above mentioned bifurcation diverts both surface water and denser intermediate water offshore into the separated EGC. Upstream of Denmark Strait the separated EGC partly merges with the North Icelandic Jet which transports water originating from intermediate depths in the Iceland Sea [*Våge et al*., 2011; *Harden et al*., 2016]. To complete the overview of the circulation in the Nordic Seas, we have also included the inflowing North Icelandic Irminger Current (NIIC) which transports Atlantic Water northward through Denmark Strait and into the Iceland Sea.

The PSW Jet, indicated as a separate current branch on the Greenland continental shelf in Figure 13, is responsible for a substantial fraction of the FWT (more than 50% in one of the three sections). Unfortunately, we have no means of evaluating whether this branch is present throughout the year. *Köhl et al*. [2007] presented a 3 year mean meridional section across the EGC close to 68°N from a numerical model where a substantial southward transport takes place on the shelf. However, they did not elaborate upon the temporal variation of this feature. Due to its origin on the Greenland shelf and its relationship to the density gradients of PSW, the PSW Jet may be most important in summer when the pool of freshwater on the shelf increases due to runoff from Greenland and ice melt. This could increase the cross-shelf density gradient and strengthen the PSW Jet.

Between section 6 and the Blosseville Basin, the total FWT of the EGC system decreased significantly, but it is not clear what caused this decrease. At least two scenarios are possible. Either the FWT could be diverted into the western Iceland Sea west of the Kolbeinsey Ridge or it could be advected into the central Iceland Sea by the East Icelandic Current. In the second scenario, the mismatch between the estimates of FWT in the EIC at the Langanes section northeast of Iceland [*Macrander et al*., 2014] and the decrease in FWT measured here suggests that, if the freshwater is transported into the Iceland Sea, it does not reach as far east as Langanes and instead penetrates into the Iceland Sea. The northwestern corner of the Iceland Sea has been identified as a possible source region for the densest waters formed by wintertime convection that supply the NIJ [*Våge et al*., 2015]. The preconditioning for convection in this area is likely influenced by the offshore diversion of both fresh surface waters and Atlantic-origin Water from the EGC. The freshwater could inhibit convection due to the increased surface stratification, or, if it takes part in convection, could be sequestered at depth. Either way the fate of the freshwater can potentially have important implications for the formation and hydrographic properties of the dense water supplying the Denmark Strait Overflow.

The shelfbreak EGC carries both light surface water from the Arctic Ocean and denser intermediate water masses. This current branch was the major source of dense water from the EGC to the Denmark Strait Overflow, with an average transport of 2.8 ± 0.7 Sv. With a nearly isopycnal along-stream modification of the Atlantic-origin Water from Fram Strait to Denmark Strait, the density of the overflow water was not very sensitive to these hydrographic changes. As a result, the presence of relatively unmodified water from Fram Strait in the northern Blosseville Basin did not affect the local density of the overflow directly. However, due to the differing effect of pressure on warm and cold water, the density at depth in the North Atlantic would be greatest for the overflow water that was most strongly modified, i.e., the coldest variant. Hence, even though a warmer and more saline overflow layer has a similar density locally, it may not reach the same equilibrium depth after crossing the sill and sinking.

With the large section-to-section variability measured in our EGC survey, it is evident that the transport estimates presented here must be treated with some caution. Nevertheless, the high-resolution hydrography and velocity observations have allowed us to present synoptic flux estimates associated with all three

branches of the EGC system, as they progress from Fram Strait to Denmark Strait. These are the first summertime estimates since the RV Oden expedition in 2002 [*Rudels et al.*, 2005; *Nilsson et al.*, 2008], and the first based on absolute geostrophic velocities. Our results have shed light on the circulation of Atlantic-origin Water in the Nordic Seas from south of Fram Strait to Denmark Strait, and, at the same time, have identified several open questions for further study.

Acknowledgments
Support for this work was provided by the Norwegian Research Council under grant agreement 231647 (L.H. and K.V.), and the European Union 7th Framework Programme (FP7 2007-2013) under grant agreement 308299 NACLIM Project (K.V.). Funding was also provided by the U.S. National Science Foundation under grant OCE-0959381 (R.P.). The data from the RRS James Clark Ross survey can be obtained from http://kogur.whoi.edu. CTD data from RV Oceania cruises can be retrieved from the IOPAN data base or requested directly from abesz@iopan.gda.pl. The data obtained from Pangaea.de were collected by the Alfred Wegner Institute and the Norwegian Polar Institute (cruises ARK XIV/2, ARK XV/3, LA97/2, LA02, LA03/12, and LA04/15).

References

Aksenov, Y., S. Bacon, A. C. Coward, and A. G. Nurser (2010), The North Atlantic inflow to the Arctic Ocean: High-resolution model study, *J. Mar. Syst.*, *79*(1–2), 1–22, doi:10.1016/j.jmarsys.2009.05.003.

Bacon, S., G. Reverdin, I. G. Rigor, and H. M. Snaith (2002), A freshwater jet on the east Greenland shelf, *J. Geophys. Res.*, *107*(C7), doi:10.1029/2001JC000935.

Bacon, S., P. G. Myers, B. Rudels, and D. A. Sutherland (2008), *Accessing the Inaccessible: Buoyancy-Driven Coastal Currents on the Shelves of Greenland and Eastern Canada*, pp. 703–722, Springer, Dordrecht, Netherlands, doi:10.1007/978-1-4020-6774-7_29.

Bacon, S., A. Marshall, N. P. Holliday, Y. Aksenov, and S. R. Dye (2014), Seasonal variability of the East Greenland Coastal Current, *J. Geophys. Res. Oceans*, *119*, 3967–3987, doi:10.1002/2013JC009279.

Beszczynska-Möller, A., E. Fahrbach, U. Schauer, and E. Hansen (2012), Variability in Atlantic water temperature and transport at the entrance to the Arctic Ocean, 1997–2010, *ICES J. Mar. Sci.*, *69*(5), 852–863, doi:10.1093/icesjms/fss056.

Bourke, R. H., A. M. Weigel, and R. G. Paquette (1988), The westward turning branch of the West Spitsbergen Current, *J. Geophys. Res.*, *93*(C11), 14,065–14,077, doi:10.1029/JC093iC11p14065.

Bourke, R. H., R. G. Paquette, and R. F. Blythe (1992), The Jan Mayen Current of the Greenland Sea, *J. Geophys. Res.*, *97*(C5), 7241–7250, doi:10.1029/92JC00150.

de Steur, L., E. Hansen, R. Gerdes, M. Karcher, E. Fahrbach, and J. Holfort (2009), Freshwater fluxes in the East Greenland Current: A decade of observations, *Geophys. Res. Lett.*, *36*, L23611, doi:10.1029/2009GL041278.

de Steur, L., E. Hansen, C. Mauritzen, A. Beszczynska-Möller, and E. Fahrbach (2014), Impact of recirculation on the East Greenland Current in Fram Strait: Results from moored current meter measurements between 1997 and 2009, *Deep Sea Res., Part I*, *92*, 26–40, doi:10.1016/j.dsr.2014.05.018.

de Steur, L., R. S. Pickart, D. J. Torres, and H. Valdimarsson (2015), Recent changes in the freshwater composition east of Greenland, *Geophys. Res. Lett.*, *42*, 2326–2332, doi:10.1002/2014GL062759.

Dickson, R. R., and J. Brown (1994), The production of North Atlantic Deep Water: Sources, rates, and pathways, *J. Geophys. Res.*, *99*(C6), 12,319–12,341, doi:10.1029/94JC00530.

Egbert, G. D., and S. Y. Erofeeva (2002), Efficient inverse modeling of barotropic ocean tides, *J. Atmos. Oceanic Technol.*, *19*(2), 183–204, doi:10.1175/1520-0426(2002)019 < 0183:EIMOBO > 2.0.CO;2.

Fahrbach, E., J. Meincke, S. Østerhus, G. Rohardt, U. Schauer, V. Tverberg, and J. Verduin (2001), Direct measurements of volume transports through Fram Strait, *Polar Res.*, *20*(2), 217–224, doi:10.1111/j.1751-8369.2001.tb00059.x.

Haine, T. W., et al. (2015), Arctic freshwater export: Status, mechanisms, and prospects, *Global Planet. Change*, *125*, 13–35, doi:10.1016/j.gloplacha.2014.11.013.

Hansen, B., and S. Østerhus (2000), North Atlantic-Nordic Seas exchanges, *Prog. Oceanogr.*, *45*(2), 109–208, doi:10.1016/S0079-6611(99)00052-X.

Hansen, B., K. M. H. Larsen, H. Hátún, R. Kristiansen, E. Mortensen, and S. Østerhus (2015), Transport of volume, heat, and salt towards the Arctic in the Faroe Current 1993–2013, *Ocean Sci.*, *11*(5), 743–757, doi:10.5194/os-11-743-2015.

Hansen, E. (2006a), *Physical Oceanography During LANCE Cruise LA02*, Norw. Polar Inst., Tromsø, Norway, doi:10.1594/PANGAEA.512016.

Hansen, E. (2006b), *Physical Oceanography During LANCE Cruise LA03/12*, Norw. Polar Inst., Tromsø, Norway, doi:10.1594/PANGAEA.524746.

Hansen, E. (2006c), *Physical Oceanography During LANCE Cruise LA04/15*, Norw. Polar Inst., Tromsø, Norway, doi:10.1594/PANGAEA.525956.

Harden, B. E., I. A. Renfrew, and G. N. Petersen (2011), A climatology of wintertime barrier winds off southeast Greenland, *J. Clim.*, *24*(17), 4701–4717, doi:10.1175/2011JCLI4113.1.

Harden, B. E., et al. (2016), Upstream sources of the Denmark Strait Overflow: Observations from a high-resolution mooring array, *Deep Sea Res., Part I*, *112*, 94–112, doi:10.1016/j.dsr.2016.02.007.

Hattermann, T., P. E. Isachsen, W.-J. von Appen, J. Albretsen, and A. Sundfjord (2016), Eddy-driven recirculation of Atlantic Water in Fram Strait, *Geophys. Res. Lett.*, *43*, 3406–3414, doi:10.1002/2016GL068323.

Holfort, J., and J. Meincke (2005), Time series of freshwater-transport on the East Greenland Shelf at 74°N, *Meteorol. Z.*, *14*(6), 703–710, doi:10.1127/0941-2948/2005/0079.

Holfort, J., E. Hansen, S. Østerhus, S. Dye, S. Jónsson, J. Meincke, J. Mortensen, and M. Meredith (2008), *Freshwater Fluxes East of Greenland*, pp. 263–287, Springer, Dordrecht, Netherlands, doi:10.1007/978-1-4020-6774-7_12.

Isachsen, P. E., C. Mauritzen, and H. Svendsen (2007), Dense water formation in the Nordic Seas diagnosed from sea surface buoyancy fluxes, *Deep Sea Res., Part I*, *54*(1), 22–41, doi:10.1016/j.dsr.2006.09.008.

Jeansson, E., S. Jutterström, B. Rudels, L. G. Anderson, K. A. Olsson, E. P. Jones, W. M. Smethie, and J. H. Swift (2008), Sources to the East Greenland Current and its contribution to the Denmark Strait Overflow, *Prog. Oceanogr.*, *78*(1), 12–28, doi:10.1016/j.pocean.2007.08.031.

Jochumsen, K., D. Quadfasel, H. Valdimarsson, and S. Jónsson (2012), Variability of the Denmark Strait overflow: Moored time series from 1996–2011, *J. Geophys. Res.*, *117*, C12003, doi:10.1029/2012JC008244.

Köhl, A., R. H. Käse, D. Stammer, and N. Serra (2007), Causes of changes in the Denmark Strait Overflow, *J. Phys. Oceanogr.*, *37*(6), 1678–1696, doi:10.1175/JPO3080.1.

Lilly, J. M., P. B. Rhines, F. Schott, K. Lavender, J. Lazier, U. Send, and E. D'Asaro (2003), Observations of the Labrador Sea eddy field, *Prog. Oceanogr.*, *59*(1), 75–176, doi:10.1016/j.pocean.2003.08.013.

Macrander, A., H. Valdimarsson, and S. Jónsson (2014), Improved transport estimate of the East Icelandic Current 2002–2012, *J. Geophys. Res. Oceans*, *119*, 3407–3424, doi:10.1002/2013JC009517.

Manley, T. O. (1995), Branching of Atlantic Water within the Greenland-Spitsbergen Passage: An estimate of recirculation, *J. Geophys. Res.*, *100*(C10), 20,627–20,634, doi:10.1029/95JC01251.

Marnela, M., B. Rudels, M.-N. Houssais, A. Beszczynska-Möller, and P. B. Eriksson (2013), Recirculation in the Fram Strait and transports of water in and north of the Fram Strait derived from CTD data, *Ocean Sci.*, *9*(3), 499–519, doi:10.5194/os-9-499-2013.

Mauritzen, C. (1996), Production of dense overflow waters feeding the North Atlantic across the Greenland-Scotland Ridge: Part 1: Evidence for a revised circulation scheme, *Deep Sea Res., Part I*, *43*(6), 769–806, doi:10.1016/0967-0637(96)00037-4.

Nilsson, J., G. Björk, B. Rudels, P. Winsor, and D. Torres (2008), Liquid freshwater transport and Polar Surface Water characteristics in the East Greenland Current during the AO-02 Oden expedition, *Prog. Oceanogr.*, *78*(1), 45–57, doi:10.1016/j.pocean.2007.06.002.

Nurser, A. J. G., and S. Bacon (2014), The Rossby radius in the Arctic Ocean, *Ocean Sci.*, *10*(6), 967–975, doi:10.5194/os-10-967-2014.

Orvik, K. A., and P. Niiler (2002), Major pathways of Atlantic water in the northern North Atlantic and Nordic Seas toward Arctic, *Geophys. Res. Lett.*, *29*(19), 1896, doi:10.1029/2002GL015002.

Paquette, R. G., R. H. Bourke, J. F. Newton, and W. F. Perdue (1985), The East Greenland Polar Front in autumn, *J. Geophys. Res.*, *90*(C3), 4866–4882, doi:10.1029/JC090iC03p04866.

Pickart, R. S., and W. M. Smethie (1998), Temporal evolution of the deep western boundary current where it enters the sub-tropical domain, *Deep Sea Res., Part I*, *45*(7), 1053–1083, doi:10.1016/S0967-0637(97)00084-8.

Quadfasel, D., J.-C. Gascard, and K.-P. Koltermann (1987), Large-scale oceanography in Fram Strait during the 1984 Marginal Ice Zone Experiment, *J. Geophys. Res.*, *92*(C7), 6719–6728, doi:10.1029/JC092iC07p06719.

Rabe, B., U. Schauer, A. Mackensen, M. Karcher, E. Hansen, and A. Beszczynska-Möller (2009), Freshwater components and transports in the Fram Strait—Recent observations and changes since the late 1990s, *Ocean Sci.*, *5*(3), 219–233, doi:10.5194/os-5-219-2009.

Rabe, B., et al. (2013), Liquid export of Arctic freshwater components through the Fram Strait 1998–2011, *Ocean Sci.*, *9*(1), 91–109, doi:10.5194/os-9-91-2013.

Rudels, B., E. Fahrbach, J. Meincke, G. Budèus, and P. Eriksson (2002), The East Greenland Current and its contribution to the Denmark Strait overflow, *ICES J. Mar. Sci.*, *59*(6), 1133–1154, doi:10.1006/jmsc.2002.1284.

Rudels, B., G. Björk, J. Nilsson, P. Winsor, I. Lake, and C. Nohr (2005), The interaction between waters from the Arctic Ocean and the Nordic Seas north of Fram Strait and along the East Greenland Current: Results from the Arctic Ocean-02 Oden expedition, *J. Mar. Syst.*, *55*(1), 1–30, doi:10.1016/j.jmarsys.2004.06.008.

Schauer, U. (2010), *Physical Oceanography During POLARSTERN Cruise ARK-XV/3*, Alfred Wegener Inst., Helmholtz Cent. for Polar and Mar. Res., Bremerhaven, Germany, doi:10.1594/PANGAEA.742657.

Schauer, U., and G. Budéus (2010), *Physical Oceanography During POLARSTERN Cruise ARK-XIV/2*, Alfred Wegener Inst., Helmholtz Cent. for Polar and Mar. Res., Bremerhaven, Germany, doi:10.1594/PANGAEA.742655.

Schauer, U., and G. Rohardt (2010), *Physical Oceanography During LANCE Cruise LA97/2*, Alfred Wegener Inst., Helmholtz Cent. for Polar and Mar. Res., Bremerhaven, Germany, doi:10.1594/PANGAEA.742622.

Seidov, D., et al. (2015), Oceanography north of 60°N from World Ocean Database, *Prog. Oceanogr.*, *132*, 153–173, doi:10.1016/j.pocean.2014.02.003.

Spall, M. A. (1995), Frontogenesis, subduction, and cross-front exchange at upper ocean fronts, *J. Geophys. Res.*, *100*(C2), 2543–2557, doi:10.1029/94JC02860.

Strass, V. H., E. Fahrbach, U. Schauer, and L. Sellmann (1993), Formation of Denmark Strait Overflow Water by mixing in the East Greenland Current, *J. Geophys. Res.*, *98*(C4), 6907–6919.

Sutherland, D. A. (2008), The East Greenland Coastal Current: Its structure variability, and large-scale impact, PhD thesis, Mass. Inst. of Technol. and Woods Hole Oceanogr. Inst., Woods Hole.

Sutherland, D. A., and R. S. Pickart (2008), The East Greenland Coastal Current: Structure, variability, and forcing, *Prog. Oceanogr.*, *78*(1), 58–77, doi:10.1016/j.pocean.2007.09.006.

Våge, K., R. S. Pickart, M. A. Spall, H. Valdimarsson, S. Jónsson, D. J. Torres, S. Østerhus, and T. Eldevik (2011), Significant role of the North Icelandic Jet in the formation of Denmark Strait Overflow Water, *Nat. Geosci.*, *4*(10), 723–727, doi:10.1038/NGEO1234.

Våge, K., R. S. Pickart, M. A. Spall, G. Moore, H. Valdimarsson, D. J. Torres, S. Y. Erofeeva, and J. E. Ø. Nilsen (2013), Revised circulation scheme north of the Denmark Strait, *Deep Sea Res., Part I*, *79*, 20–39, doi:10.1016/j.dsr.2013.05.007.

Våge, K., G. Moore, S. Jónsson, and H. Valdimarsson (2015), Water mass transformation in the Iceland Sea, *Deep Sea Res., Part I*, *101*, 98–109, doi:10.1016/j.dsr.2015.04.001.

von Appen, W.-J., and R. S. Pickart (2012), Two configurations of the Western Arctic Shelfbreak Current in summer, *J. Phys. Oceanogr.*, *42*(3), 329–351, doi:10.1175/JPO-D-11-026.1.

von Appen, W.-J., U. Schauer, T. Hattermann, and A. Beszczynska-Möller (2016), Seasonal cycle of mesoscale instability of the West Spitsbergen Current, *J. Phys. Oceanogr.*, *46*(4), 1231–1254, doi:10.1175/JPO-D-15-0184.1.

Walczowski, W. (2013), Frontal structures in the West Spitsbergen Current margins, *Ocean Sci.*, *9*(6), 957–975, doi:10.5194/os-9-957-2013.

Walczowski, W., and J. Piechura (2007), Pathways of the Greenland Sea warming, *Geophys. Res. Lett.*, *34*, L10608, doi:10.1029/2007GL029974.

Woodgate, R. A., E. Fahrbach, and G. Rohardt (1999), Structure and transports of the East Greenland Current at 75°N from moored current meters, *J. Geophys. Res.*, *104*(C8), 18,059–18,072, doi:10.1029/1999JC900146.